

Detection, Discrimination and Real-Time Tracking of Cracks in Rotating Disks

Wayne C. Haase, Ph.D.

Aerogage Corp, 7 Matthew Lane, Sterling MA 01564 978 422-8224, waynehaase@aerogage.com

Michael J. Drumm

ExSell inc., 964 Autumn Oak Circle, Concord CA 94521 925 685-0227 mdrumm@exsellinc.com

Abstract—The purpose of this effort was to develop a system* to detect, discriminate and track fatigue cracks in rotating disks. Aimed primarily at jet engines in flight applications, the system also has value for detecting cracks in a spin pit during low cycle fatigue testing, and for monitoring the health of steam turbines and land-based gas turbine engines for maintenance purposes.

The results of this effort produced: a physics-based model that describes the change in the center of mass of a rotating disk using damping ratio, initial unbalance and crack size as parameters; the development of a data acquisition and analysis system that can detect and discriminate a crack using a single cycle of data; and initial validation of the model through testing in a spin pit.

The development of the physics-based model also pointed to the most likely regimes for crack detection; identified specific powers of ω to search for in specific regimes; dictated a particular type of data acquisition for crack discrimination; and demonstrated a need for a higher signal-to-noise ratio in the measurement of the basic vibration signal.

TABLE OF CONTENTS

1. ABSTRACT
2. INTRODUCTION
3. PHYSICS-BASED MODEL
4. OUTLINE OF NEW CRACK DETECTION METHOD
5. TEST RESULTS
6. SUMMARY

1. INTRODUCTION

When disks are rotated at high speed, centrifugal force produces a stress that results in a finite strain or growth of the disk. If stressed within its elastic region the disk material returns to its original size when the stress is removed, but if the stress (or speed of rotation) was of sufficient magnitude, a small but finite portion of the disk life is consumed. Additional cycles (excursions from low speed to high speed back to low speed) consume incremental portions of the disk life until the material fatigues and a crack(s) initiates, propagates and ultimately causes the disk to burst. This is the source of Low Cycle Fatigue in aircraft components, steam turbines, flywheels,

medical centrifuges, and other high-speed rotating objects. Cracks usually start in high stress areas like dovetail slots (attachment points for disks and blades), but can occur in the disk bore, in boltholes, in the rim, or in attached blades.

Much of the effort in Non-Destructive Testing (NDT) has gone towards identifying when and where cracks have developed in rotating hardware. In a jet engine the rotating disks are inspected at regular intervals using a fluorescent penetrant, a dye that seeps into cracks and shows up as an identifiable line under ultraviolet light. Fluorescent Penetrant Inspection (FPI) is useful in detecting cracks in disks but the engine must be disassembled for inspection and subsurface cracks cannot be identified. FPI is also limited in the size of crack it can identify, and the quality of the inspection is heavily dependent on the skill of the inspector.

Other crack detection technology includes an inspection with an eddy current probe that is more sensitive than FPI, but probes must be constructed for specific areas of the disk, leaving the other areas untested. This characteristic of an eddy current probe caused the surprise burst of a large fan in a spin pit test when the areas being tested for cracks were not the area that the crack was growing in. Failures of these inspection techniques also caused the unexpected burst of disks in aircraft at Sioux City, Pensacola and other locations, resulting in fatalities among passenger and crew, and causing severe damage to aircraft.

The initiation and growth of a crack is a probabilistic event, so to increase safety and reduce uncertainty the cycle life of disks are specified substantially less than that expected for crack initiation. For example, if the burst life of a disk is 30,000 cycles, and a crack typically initiates at around 15,000 cycles, then the disk may very well be removed from service after only 8,000 cycles. Even with this conservative approach, a few disks, typically with material flaws, make it into the fleet, past the schedule of inspections, and cause injury, death and/or property damage as a result of uncontained disk bursts.

The current system of operational disk cycle counting and offline inspection produces the following results:

* Patent Pending

1. A large majority of disks are retired early with a substantial number of potential cycles remaining.
2. A very small number of bad disks still make it through the inspection process and cause uncontained disk bursts.
3. The cost of the program is enormous due to the significant waste of potentially useful flight hardware, the large cost of removing and disassembly of an engine, and the investment in inspection facilities that don't uncover all problems.

Existing real-time crack detection schemes are based on experimentation and have no analytical basis to validate from. These systems were designed to detect cracks in disks during a spin test, and measure the amplitude and phase of a difference vector that represents the change in center of mass of the disk due to a crack. The relationship of this change in center of mass to the size or dimensions of the crack is unknown, and all measurements are typically performed at a single frequency. The results that display the movement of the center of mass are very noisy due to the measurement technique, and numerous cycles are required before an indication of a crack can be identified. In addition, there is no mechanism to easily discriminate a crack from other phenomena that might cause a change in the center of mass.

This paper describes a new technique for detecting cracks in rotating structures that has an analytical basis in a model developed by ExSell, and that has been verified through testing in a spin pit. The technique allows the detection and discrimination of a crack during a single cycle by acquiring data during a speed profile and performing a crack analysis during each acceleration and/or deceleration of the disk. The model outlines different regimes where crack detection can take place, what kind of measurement sensitivity is required, and what kind of data acquisition technique is optimum for crack detection.

The model describes in detail the change in center of mass of a rotating object in a soft mount as a function of speed,

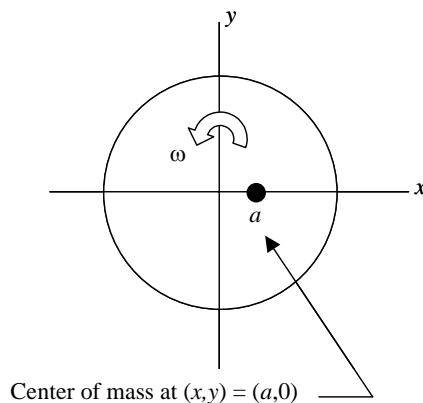


Fig. 1a

using damping ratio, initial unbalance and crack size as parameters. This model has been verified by testing of a cracked rotor in a spin pit, and future work will relate crack size to actual readings of crack growth.

2. PHYSICS-BASED MODEL

The development of a physics-based model for crack detection provided a substantial base to the work on this effort. The benefits of the developed model are:

1. It pointed to the most likely regimes for crack detection.
2. It identified specific powers of ω to search for in specific regimes.
3. It dictated a particular type of data acquisition for crack discrimination.
4. It demonstrated a need for a higher signal-to-noise ratio in the measurement of the basic vibration signal.

A description of the model and a discussion of its characteristics are given below:

When adding a crack to the rotor, assume the following (see Figures 1a & 1b):

1. The center of mass changes due to a crack opening and closing
2. The motion of the center of mass is proportional to ω^2 , with coefficient b_0 the displacement at $\omega = \omega_n$.
3. The initial offset a for the center of mass is at $\theta = 0$ (i.e. $x=a, y=0$).
4. The motion of the center of mass is at angle θ_b .

For $a = 0.001$ $r = 0.1, 0.2, \dots, 100$
 d (damping ratio) = 0.1

$$X(r,a,d) = \frac{ar^2}{\sqrt{(1-r^2)^2 + (2rd)^2}} \quad (1)$$

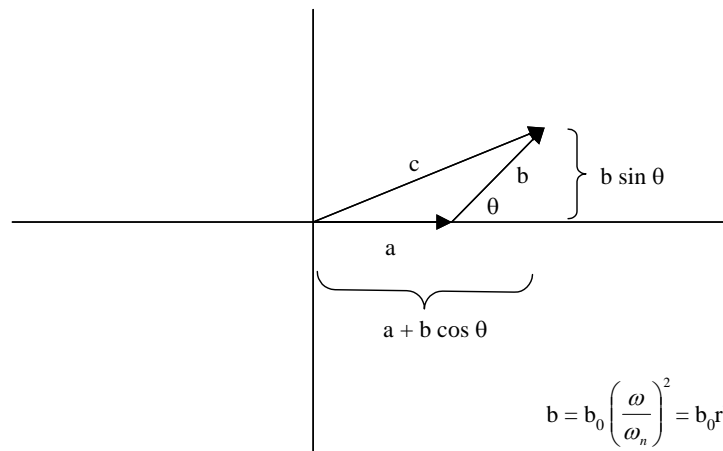


Fig. 1b

$$\theta(r,d) = \frac{180}{\pi} \operatorname{atan} \left(\frac{2rd}{1-r^2} \right) \quad (2)$$

this equation returns the principal value between $-\pi/2$ and $+\pi/2$

$$\theta_2(r,d) = \frac{180}{\pi} a \tan 2(1-r^2, 2rd) \quad (3)$$

this second equation returns the value from $-\pi$ to $+\pi$ and is preferred because it avoids ambiguities and provides a full 4-quadrant capability.

$$\text{for } \theta_b = 90^\circ \quad b_0 = 0.00001$$

$$b(r) = b_0 r^2 \quad (4)$$

$$X_c(r,a,d) = \frac{r^2 \sqrt{a^2 + b(r)^2 + 2ab(r) \cos \theta_b}}{\sqrt{(1-r^2)^2 + (2rd)^2}}$$

$$\theta(r,a,d) = \frac{180}{\pi} (-\operatorname{atan} 2(1-r^2, 2rd) + \operatorname{atan} 2(a+b(r) \cos(\theta_b), b(r) \sin(\theta_b))) \quad (5)$$

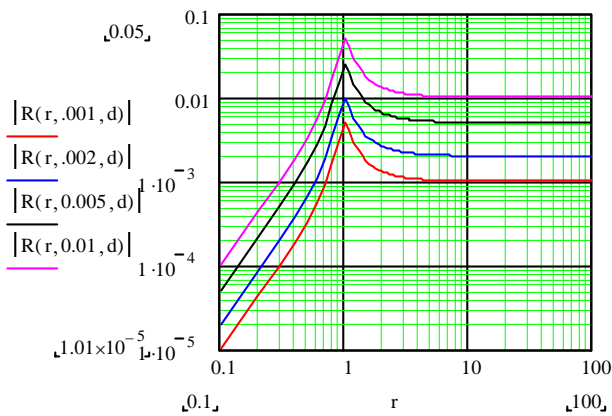


Fig. 2

Magnitude of shaft displacement as a function of RPM on a log-log scale, for different values of initial unbalance of the system. The curves in Fig. 2 are similar to two-bearing Jeffcott rotor solutions found in standard texts.

These two formulas represent the magnitude and phase of the displacement of the spindle for a disk with a crack that is vertically hung in a soft mount.

Figure 2 plots the displacement of the shaft as a function of RPM on a log-log scale for different values of the initial unbalance of the system. At $\omega=0$ the displacement would be $r=0$. As ω increases, the displacement of the shaft (and the center of mass) increases until the system reaches the critical frequency, RPM-critical ($r=1$). The graph shows that

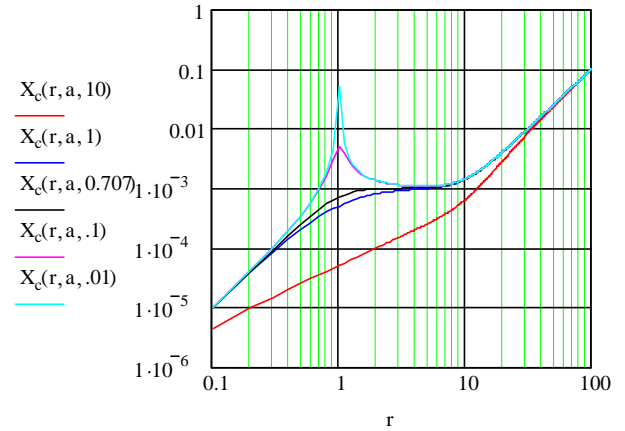


Fig. 3

Magnitude of shaft displacement of a disk with a crack, using damping ratio as a parameter

below critical the increase is proportional to ω^2 . At the critical frequency, the displacement is bounded by the damping of the system. As ω increases above the critical frequency, the sign of the displacement changes and the mass tries to rotate about its own center of mass. As ω approaches infinity, the displacement x approaches the value of "a" the initial misalignment of the center of mass.

Figure 3 is a graph of the magnitude of the shaft displacement of a disk with a crack, using damping ratio as a parameter. The graph shows that below first critical (at $r=1$), for all conditions except for the heavily over-damped case, the motion of the center of mass increases at a rate proportional to ω^2 . Above the critical frequency, the position of the center of mass approaches the value of "a" (the initial offset between the center of mass and the geometric center of the rotor), but as ω continues to increase, the center of mass begins to follow the change due to the crack. At this point, the change in the center of mass is again proportional to ω^2 . If the crack were not present, there would be no change in the position of the center of mass (as shown previously).

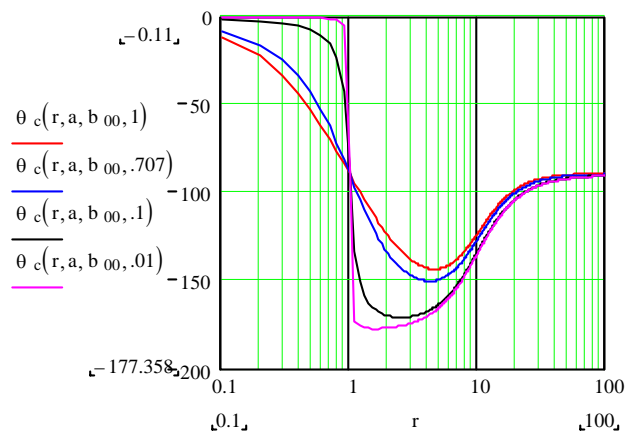


Fig. 4. Phase of magnitudes of shaft displacements for disk with a crack.

Figure 4 is a plot of the angle or phase of the magnitudes of shaft displacements for a disk with a crack as shown in Figure 3. At high values of ω , the angle approaches the negative of the angle associated with the crack. That is, if the crack causes the center of mass to move in a particular direction, the rotor moves in the opposite direction so that the new location of the center of mass is at the center of rotation.

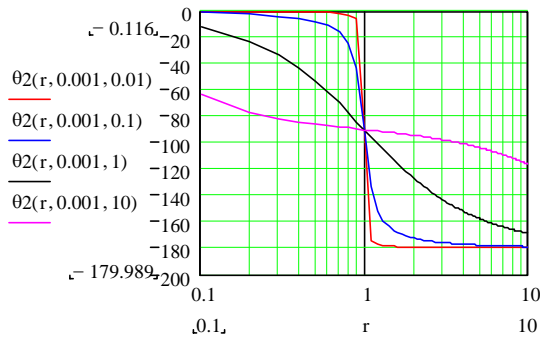


Fig. 5

Phase of response for different values of damping ratio, for disk without a crack

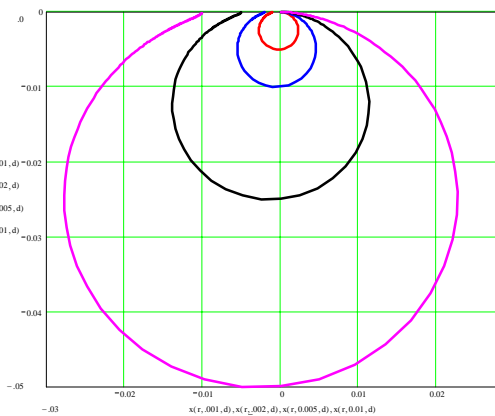


Fig. 6

Trajectory of the geometric center of the disk through critical frequency and beyond for a disk with no crack.

Fig. 5 shows the angle of the response for different values of damping ratio without a crack. Note that the angle is independent of a , the initial misalignment of the center of mass. Fig. 5 gives the angle in terms of $-\pi$ to π and shows that as r approaches infinity (ω approaches infinity), the angle of the response is 180° .

Thus, at high frequencies, when the center of mass is at 0° (on the x-axis), the displacement of the center of rotation is at 180° . Since the amplitude is equal to a (the misalignment), the center of mass is the center of rotation.

Figure 6 shows the trajectory of the geometric center of a disk, given an initial offset a , for a disk with no crack. Looking at the outside (magenta) circle, the geometric center starts at $0,0$ and moves clockwise around the circle from 0° . The large magnitude at -90° is the critical frequency and shows the effect of the damping ratio. By the time the curve has reached -180° it is well past the critical frequency and has reached the initial unbalance point, a . At this point, the actual center of mass is situated at $0,0$; the disk is physically rotating about its center of mass, and the spindle is deflected to the left an amount a , which is the magnitude of the initial unbalance.

Figure 7 shows the trajectory of the geometric center of a disk with a radial crack at $+30^\circ$, causing the center of mass to move to -150° . Once past critical frequency the crack starts to dominate and the change in the center of mass due to the crack takes the orbit of the geometric center off on a line that points toward the direction of the crack.

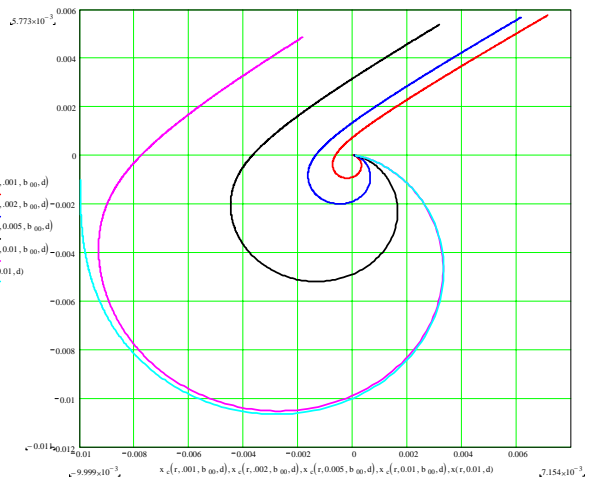


Fig. 7

Trajectory of the geometric center of the disk through critical frequency and beyond for a disk with a crack.

When the RPM gets high enough that the change in center of mass due to the crack exceeds the fixed imbalance, the crack dominates and the change in center of mass is proportional to ω^2 above first critical and proportional to ω^4 below first critical. Below that RPM the imbalance dominates and the change in center of mass follows the curve that would occur if no crack were present.

If the change in center of mass as a function of frequency can be initially measured when no crack is present, and assuming that the damping ratio and the imbalance do not change, this "baseline signature" can be subtracted from the system response. The difference between the signature obtained when a crack is present and the baseline signature may allow crack detection even below the RPM at which the crack begins to dominate.

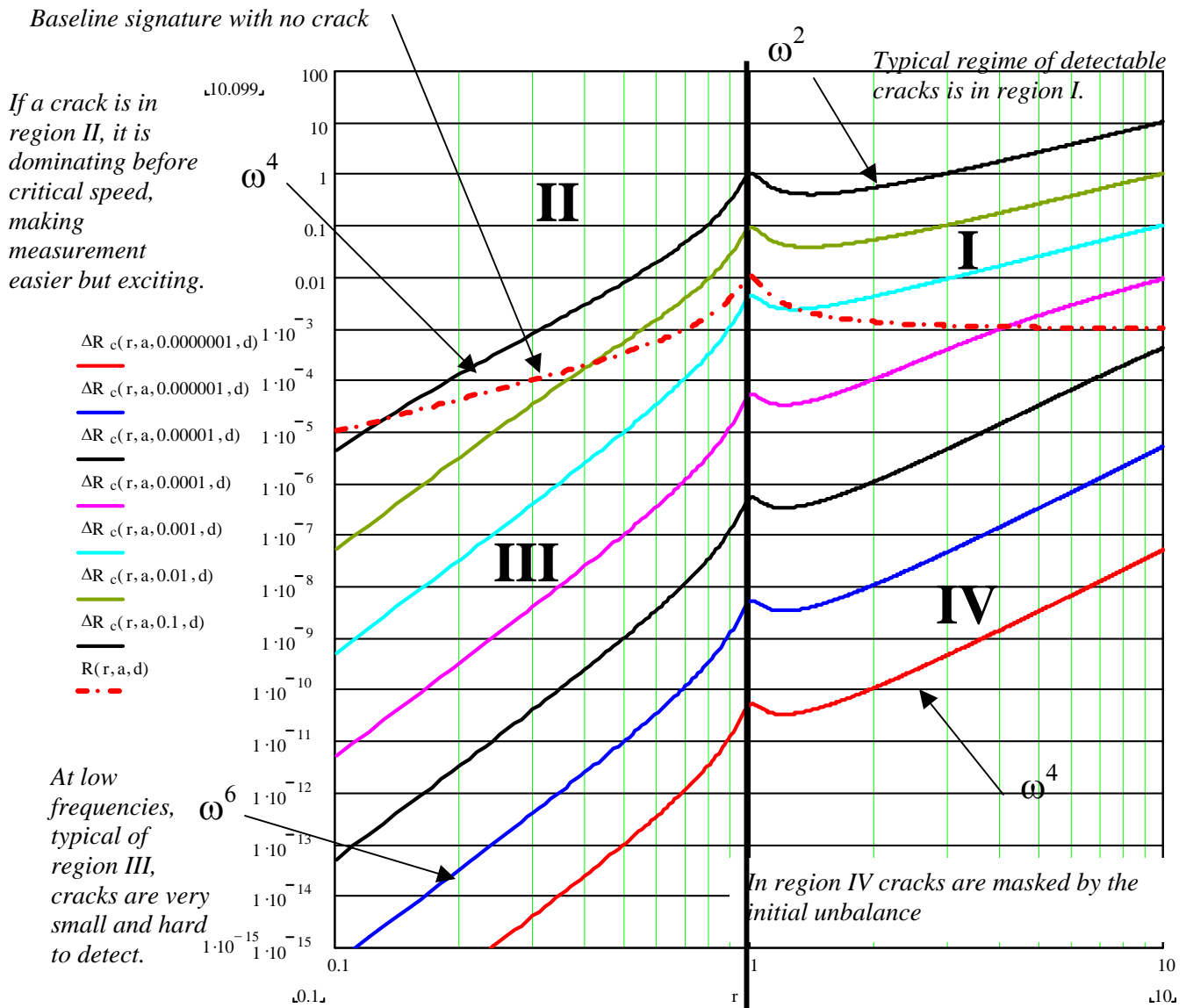


Fig. 8

Difference between the measured signature and the baseline signature for a fixed imbalance of 0.001, fixed damping ratio of 0.1, and variable crack size. The system's baseline signature for the same imbalance and damping ratio (without a crack) is shown in heavy dotted red.

Figure 8 shows the difference between the measured signature and the baseline signature for a fixed imbalance of 0.001, fixed damping ratio of 0.1, and variable crack size. The plot also shows the system's baseline signature for the same imbalance and damping ratio (without a crack).

Note that there are at least four distinct regions in which the difference between the crack signature and the baseline signature follow a different exponent in ω .

Regions I and IV are separated from regions II and III by a vertical line at the critical frequency. Regions I and II are separated from regions III and IV by the line designated Baseline Signature with No Crack.

For Region 1 (above first critical and for response dominated by a crack, or 0.001 in the above plot), the change in center of mass is proportional to ω^2 .

For Region 2 (below first critical and for response dominated by the crack), the change in center of mass is proportional to ω^4 .

For Region 3 (below first critical and for response dominated by imbalance), the change in center of mass is proportional to ω^6 .

For Region 4 (above first critical but for response dominated by imbalance, or below 0.001 in the above plot), the change in center of mass is proportional to ω^4 .

Clearly Region 1 provides the best region for crack detection because the system has an increasing change in center of mass beyond what would occur due to a fixed imbalance; furthermore, the system is above first critical so resonances due to less than critical damping are minimized.

Pushing crack detection beyond Region 1 will depend on a number of issues. The ability of a crack detection system to identify the existence of a crack, especially if the imbalance dominates the system signature, will depend on the signal-to-noise ratio of the measurement system as well as the stability of the baseline signature. Since the damping of the mechanical system has the largest effect near first critical, any change in damping (e.g. temperature changes) will make crack detection difficult near first critical. Since the signature difference is extremely small below first critical (in part due to the large exponent in ω in Region 3 and Region 2), crack detection below first critical will also be quite difficult unless the crack is so large that the crack dominates the imbalance (i.e., unless the system is in Region 2). The most promising region for extending crack detection beyond Region 1 is Region 4, particularly if the baseline signature is stable.

3. OUTLINE OF NEW CRACK DETECTION METHOD

The new method developed for crack detection is summarized below:

1. Data acquisition uses a speed profile instead of relying on readings from a constant frequency. This allows for both detection and discrimination of cracks by interpreting the speed profile using power functions of the angular velocity over a single cycle.
2. The baseline speed profile (without a crack, or initial condition) is subtracted from the current speed profile.
3. Acquisition of data from a sensor at the edges of the disk (or blade tips) is preferable to measuring the vibration of the spindle. Both techniques allow for detection of cracks, but acquiring data from the blade tips incorporates information about the movement of blades, the size increase of the disk, and can better resolve issues of center of mass movement due to multiple cracks.
4. Taking measurements at a constant frequency (usually close to the top speed of the disk) and confining measurements to Region 1 limits the size of crack that can be detected. Using a full speed profile Region IV can be explored for smaller cracks by increasing the signal-to-noise ratio of the measurement.

Test Results

A test of a 3-stage compressor stack of a military gas turbine engine started in early August, 2001 at NAVAIR in Patuxent River, MD. The test article consists of Stage 1, 2 and 3 of a compressor stack with Stage 1 on top and Stage 3 on the bottom. Stage 1 & 2 are bladed, while Stage 3 is

completely unbladed (no dummy blades). Figure 9 is a rendering of the compressor stack attached to a spin pit lid.

ExSell is making measurements on Stage 1 & 2, but Stage 2 has a long blade that makes it difficult to get clean, accurate measurements on the other blades, so the primary test for crack detection is concentrating on Stage 1. The third probe is being used as a backup. The capacitive probes were manufactured by Capacitec, in Ayer MA, and are mounted on the oven in a probe holder, measuring the gap between the end of the probe and the individual rotating blade tips.

Figure 10 is an outside view of the oven (with the compressor stack inside), which is attached to the spin pit lid. The three probes protrude out from the right side. The ExSell preamps are mounted on the top of the spin chamber, next to the lid where the probe wires exit the chamber. Wire runs then take the signals to a control room.

Figures 11 – 14 are graphs taken from the crack detection system at various cycle counts. Most important are three graphs (described below) on the right side of each display screen that show the difference vector representing the change in center of mass (from top to bottom):

- a. The magnitude and phase in an x-y format.
- b. The magnitude as a function of RPM.
- c. The phase as a function of RPM.

All graphs show both the acceleration and deceleration curves. These screens show the software development effort undertaken to revamp the crack detection software to follow the speed profile strategy shown in the model, rather than taking data only at a fixed frequency.

4. SUMMARY

This was an initial effort to advance the state of the art of crack detection beyond the experimentation stage and put the technology on a firm analytical base. The results of this effort produced: a physics-based model that describes the change in the center of mass of a rotating disk using damping ratio, initial unbalance and crack size as parameters. The effort also developed a method for detecting and discriminating a crack using a single cycle of data, and produced software and hardware for a data acquisition and analysis system for crack detection. The method was then validated through testing in a spin pit.

The development of the physics-based model for crack detection also produced additional benefits:

- a. It pointed to the most likely regimes for crack detection;
- b. It identified specific powers of ω to search for in specific regimes;
- c. It dictated a particular type of data acquisition for crack discrimination; and
- d. It demonstrated a need for a higher signal-to-noise ratio in the measurement of the basic vibration signal.

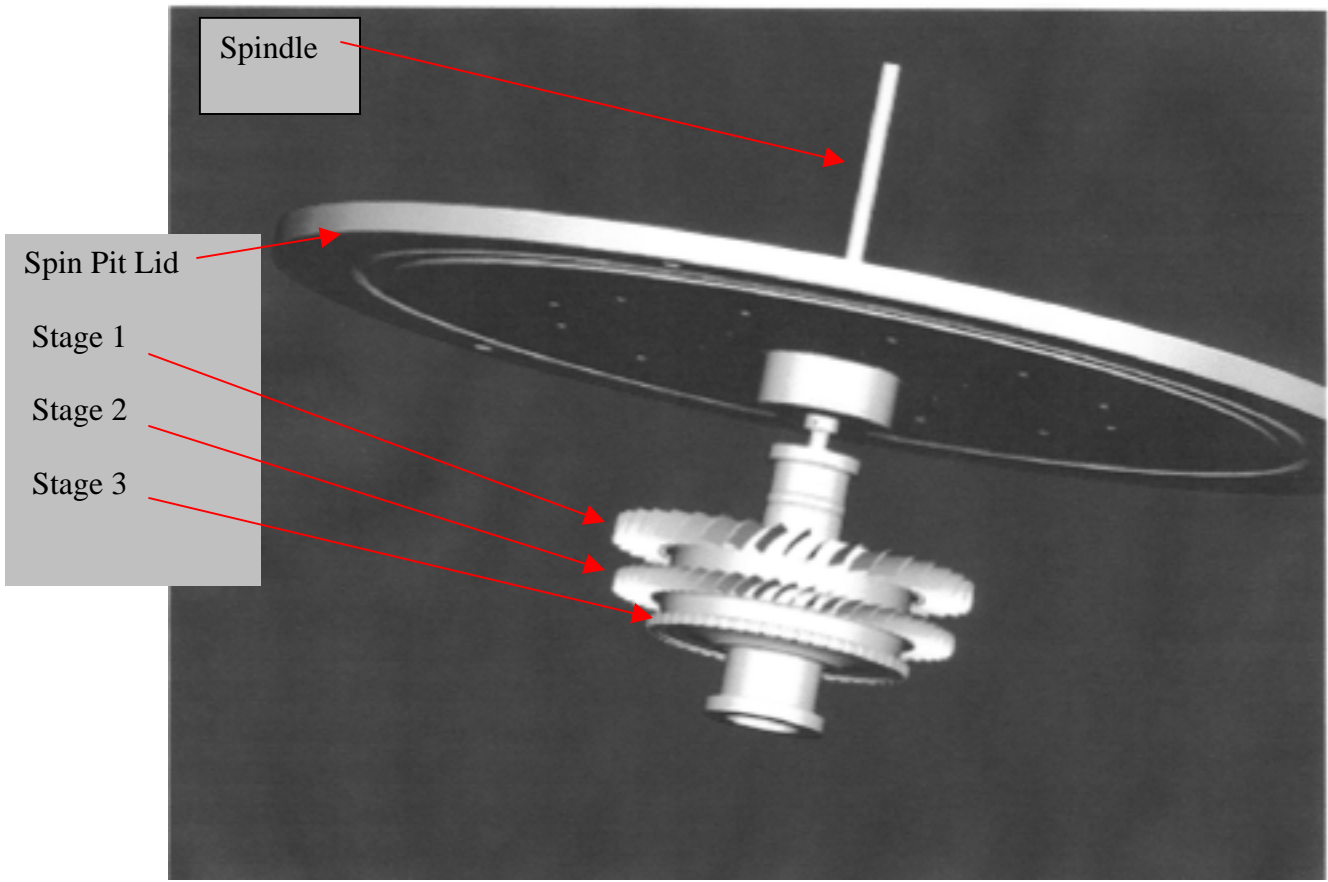


Fig. 9
 Rendering of Compressor Stack Attached to Spin Pit Lid



Fig. 10
 Outside of oven (designed by engineers at the US Navy Rotor Spin Facility and holding the compressor stack inside) attached to spin pit lid.

- Capacitec probes held by ExSell probe holders protrude from oven at right.*
- Spin pit is located at US Navy Rotor Spin Facility in Patuxent River MD.*
- Spin Pit Lid
- Three Probes
- Oven

Speed profile RPM graphs.
Plots RPM vs. RPM Counts, or
time. An RPM Count is a data
acquisition at a particular
RPM.

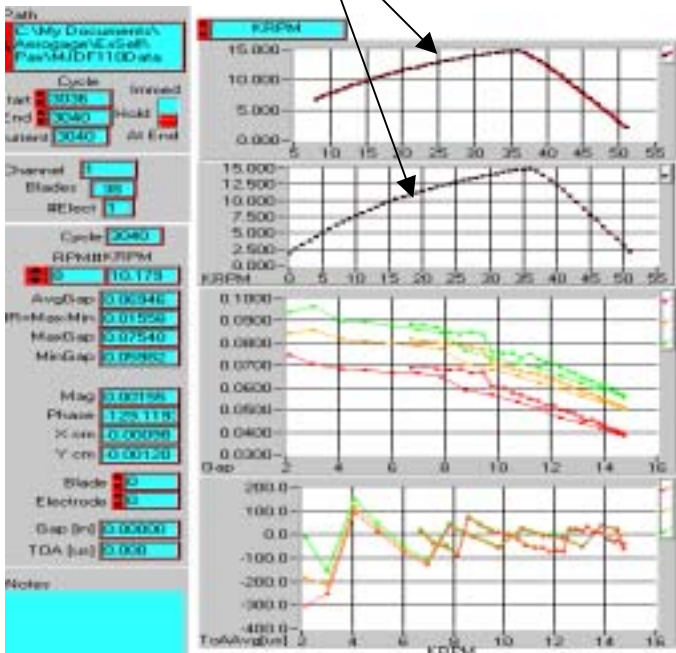
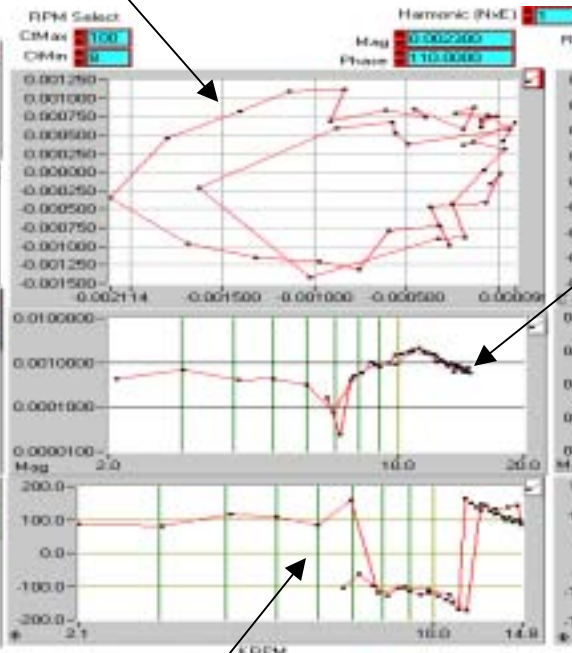


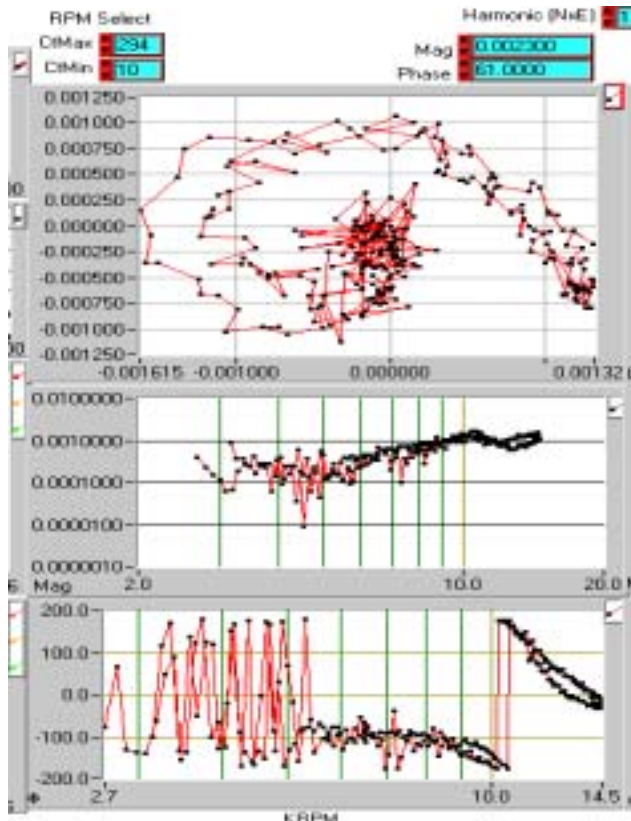
Fig. 11
Cycle 3040 Of Compressor Spin Test

Magnitude and phase in x-y format. Note the
resemblance to Figure 6 with no crack.



Phase of change of center of
mass. Compare with Fig. 5 no
crack.

Graph of
magnitude vs.
K RPM. Note
peak at
critical freq.
(11 – 12 K
RPM), then
beginning to
settle out.
Max speed is
close to
critical freq.
so the
damping ratio
also keeps the
curve from
flattenint.
Compare to
Fig. 2 with no
crack.

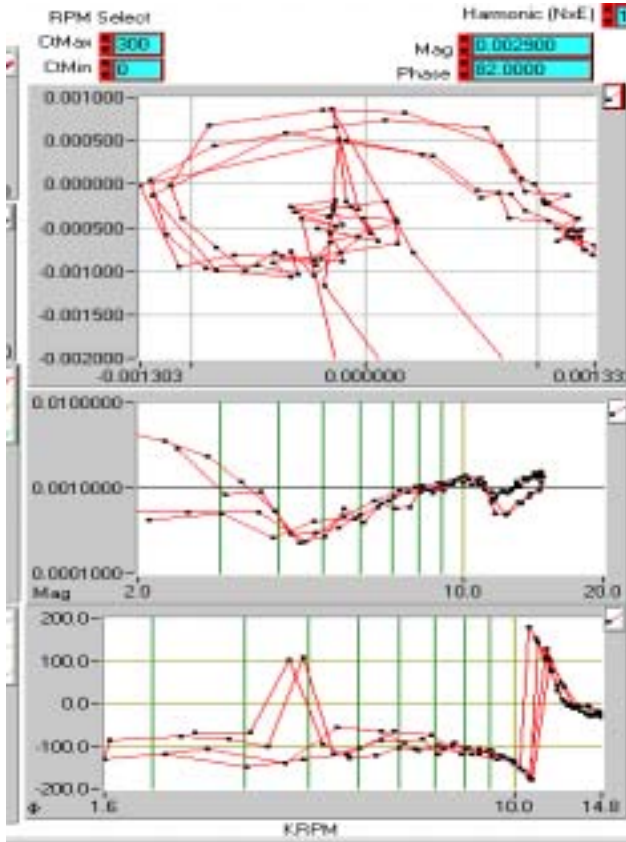


Concentrating on the crack detection
graphs, these are for cycle 3112, only
72 cycles after Figure 11.

Note how the mag-phase graph no
longer represents an almost complete
circle, and wraps around itself similar
to Fig. 7. This is the first indication of
a crack growing and is detected from
the plot of a single cycle worth of data.

At the same time the magnitude graph
has started an ω^2 rise after settling
past the critical frequency. See Fig. 3
for a representation of this in the
model. This movement of the
magnitude is also a significant
indication of a crack growing.

Fig. 12
Cycle 3112 Of Compressor Spin Test



This graph shows that the crack has grown slightly by examination of the x-y plot. The initial circle is much smaller, which is caused by the growth of the crack, and the tail is longer and more defined.

The magnitude plot still shows an ω^2 indication of a crack past the critical speed.

Fig. 13
Cycle 10.372 Of Compressor Spin Test

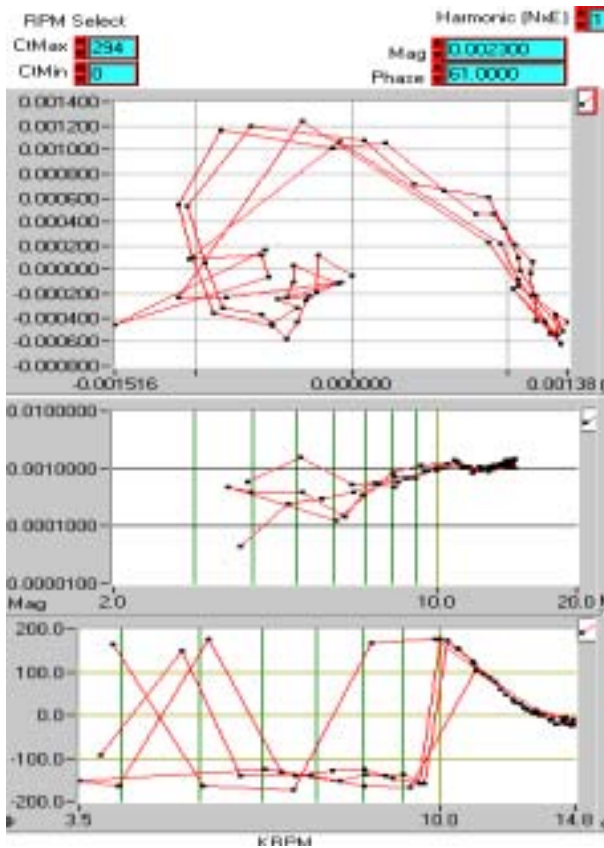


Fig. 14
Cycle 21,201 Of Compressor Spin Test

At 21,201 cycles the curves are still displaying a tightening of the x-y circle plot, and the x-y tail is pointing toward a crack (assuming it is a radial type).

The magnitude plot is still showing a crack, but with little growth.

REFERENCES

- [1] Patent # 5,533,400 Process for early detection of a crack in a rotating shaft. Gasch, Robert, Carl Schenck, AG.
- [2] Patent # 5,258,923 System and method for detecting the occurrence, location and depth of cracks in turbine-generator rotors. Imdad Imam, GE
- [3] Patent # 4,751,657 Method and apparatus for detecting axial cracks in rotors for rotating
- [4] machinery. Imdad Imam, GE
- [5] Patent # 4,408,294 Method for on-line detection of incipient cracks in turbine generator rotors. Imdad Imam, GE
- [6] Patent # 4,380,172 On-line Crack Detection, Imdad Imam, GE
- [7] W.D. Marscher, "Modal Testing of Rotating Machinery While It Is Operating", Proceedings Structural Dynamics Conference, 1997, p263
- [8] L. Hermans and H. Van der Auweraer, "Modal Testing and Analysis of Structures Under Operational Conditions", LMS International, Belgium, 2001.

Dr. Wayne C. Haase is president of Aerogage Corp. He has a Ph.D. in Electrical Engineering from Stanford Univ., and Degree of Electrical Engineer, MSEE and BSEE from MIT. Dr. Haase holds 10 patents, has been granted three National Technical Awards and has published 20 technical articles in a variety of fields.

Mr. Michael J. Drumm is President & CEO of ExSell inc. He has a BSEE from Arizona State University, has published seven technical articles in various fields, and has two patents pending.